

Integration of Lithography and Etch Simulations

Z. Krivokapic, W.D. Heavlin, and D.S. Bang

Advanced Micro Devices
P.O. Box 3453, MS 117, Sunnyvale, CA 94088, USA

Abstract

In this work we report on predictions of final gate critical dimensions using lithography and plasma etch simulators integrated with a statistical simulator.

1. Introduction

For sub 200 nm technologies, gate critical dimensions (CDs) are the dominate source of variation. Therefore, it is of paramount importance both to control CDs as tightly as possible and to understand which processing steps increase variations and by how much. Understanding the total patterning process, including the cumulative effect of lithography and etch and its manufacturability, is essential.

Our approach consists of the following elements: (a) combined Prolith 5.0, HPEM, and SPEEDIE 3.0 process simulators, (b) problem partition among simulators and calibration stages, (c) orthogonal array based Latin hypercube designs[1], (d) explicit simulator-to-empirical data calibration[2]; (e) multivariate interpolation (kriging)[3]. Regarding HPEM and SPEEDIE 3.0, their synergy has been previously reported[4].

2. Methodology

Ten major processing steps contribute to post-etch critical dimensions: the photolithographic parameters of focus, exposure dose, mask CD, photoresist thickness, Bottom Anti-Reflective Coating (BARC) thickness, development time, and Post-Exposure Bake (PEB) temperature (referred to below as L1 through L6); the etch parameters of power and overetch time (E1, E2); and wafer position, with its varying ion concentration fluxes (E3). To simulate directly using a strength-three orthogonal array requires 1000+ simulations. Further, reactor simulations are CPU-intensive, and it is beneficial to use experimental designs that minimize the number of reactor simulations. Therefore, we decouple the lithography simulator (Prolith 5.0) from the etch simulators (HPEM / SPEEDIE) and achieve a less CPU-intensive approach.

In this approach, we run the three simulators in parallel (Fig. 1). We run Prolith 5.0 against a 125-run, strength-three, six-factor Latin hypercube design[1]; its inputs are L1, ..., L6; its outputs consist of photoresist profiles—CD, slope, and thickness (Y1, Y2, Y3). For HPEM we simulate for one factor (power, E1) at five levels and observe ion fluxes along the wafer radius (E3). For SPEEDIE 3.0 we consider a 625-run, strength-four, six-

factor Latin hypercube design[1]; its input factors are Y1, Y2, Y3, E1, E2, and E3, and its measured output is the post-etch CD (Y4).

We link the input factors and the simulator outputs by applying kriging interpolation[3]. Kriging results in an implicit mathematical function that approximates a simulator output as a function of inputs, while reducing required computation. In this way, integrated predictions (of lithography through etch) become a straightforward matter of mathematical function composition.

3. Results

Using experimental data we calibrate photoresist critical dimensions and slopes and thereby to account for reticle site effects: (1) We obtain empirically measured critical dimensions of photoresist profiles (Y1') for an array of foci and exposure doses. (2) These we associate with simulator predictions. To place the results in the same range, this requires a rough offset in focus and an integer multiplier in exposure energy. Such modifications in the simulator input domain are known as "Affine Factor Transformations" (AFT)[2]. In our application, these same adjustments are common to all measured reticle sites. (3) We then form kriging models of Y1'(site) as functions of L1 (i.e. focus) and Y1; the "site" argument denotes the distinct models of each reticle site. Such post-simulator transformations are known as "Affine Response Transformations" (ART)[2]. Photoresist slopes are calibrated by replacing the predicted distribution percentiles from Prolith 5.0 with those observed empirically.

The foregoing can be summarized by the following system of equations:

$$\begin{array}{ll}
 \text{Prolith 5.0:} & Y1 = \text{DICD}(L1, \dots, L6) & Y2 = \text{SLOPE}(L1, \dots, L6) \\
 & Y3 = \text{PRTHK}(L1, \dots, L6) \\
 \text{Calibration:} & Y1'(\text{site}) = \text{DI_CAL}(L1, Y1; \text{site}) & Y2' = \text{SL_CAL}(Y2) \\
 \text{SPEEDIE/HPEM:} & Y4 = \text{FICD}(Y1', Y2, Y3, E1, E2, E3) \\
 \text{INTEGRATOR:} & Y4'(\text{site}) = \text{FICD}(Y1'(\text{site}), Y2', Y3, E1, E2, E3) \\
 & = \text{DICD}(\text{DI_CAL}(L1, \text{DICD}(L1, \dots, L6); \text{site}), \text{SL_CAL} \circ \text{SLOPE}(L1, \dots, L6), \text{PRTHK}(L1, \dots, L6), E1, E2, E3)
 \end{array}$$

All cited functions—DICD, SLOPE, ..., FICD—are kriging approximations based on the Latin hypercube experiments; the "o" operator denotes function composition.

Two different etch reactors from two different vendors are used in this study. Both use inductively coupled plasmas but with different coil configurations and different plasma power transfer characteristics. For the first reactor a chlorine chemistry (Fig 2.) is used, and for the second reactor a Cl/HBr chemistry is used (Fig. 3) [5,6].

In our study we try to predict distributions of final gate CD's for 180 nm nominal gates (Fig. 4). For the lithography part, we use a chemically enhanced photoresist exposed by conventional illumination (numerical aperture of 0.57 and partial coherence of 0.6). We use 110 nm of an organic BARC layer, and PEB is performed at 90° C. Plasma nonuniformity is modeled with the radial dependence of neutral and ion fluxes. Our assumptions are that depth of focus is 0.8 microns, exposure dose varies +/-10% (3 sigma), photoresist and BARC thickness varies 25nm, PEB temperature varies 1° C, development process varies 10%, overetch time varies 50%, and plasma reactor power varies 25%. Results of variance analysis for a pure chlorine case are presented in Table 1

for the center of the reticle field. The distribution of final CDs as a function of wafer radius is shown in Fig 5.

From Table 1, PEB temperature nonuniformity is a major source of final CD variance. In a hypothetical case when one uses photoresist that is insensitive to PEB temperature variations, the standard deviation will improve to 11.49 nm, and the 5 major variance contributors are focus at 56.7%, plasma nonuniformity at 15.8%, exposure dose at 13.8%, reactor power at 7.6%, and development at 3.3%.

4. Conclusions

Well calibrated, integrated process simulators can be used to predict the final CD distributions of etched profiles assuming all major process variations.

References

- [1] A.B. Owen, *Statistica Sinica* 2, 439, (1995).
- [2] W.D. Heavlin and L. Capodiceci, "Calibration and computer experiments," *ASA 1997 Proceedings, Section on Physical and Engineering Sciences*.
- [3] B.D. Ripley, *Spatial Statistics*, chapter 4.4, New York, Wiley, 1981.
- [4] J. Zheng, et al, *Simulation of Semiconductor Devices and Processes*, edited by H. Ryszel and P. Pichler, (Springer-Verlag, Vienna, 1995), p. 170.
- [5] M.J. Grapperhaus and M.J. Kushner, *J. Appl. Phys.* 81, 569, (1997).
- [6] W.L. Morgan, Kinema Research and Software, 1997.

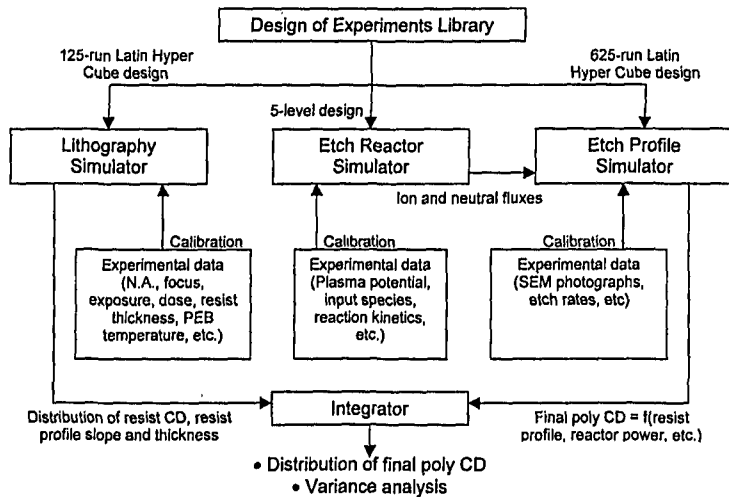


Figure 1: The chart flow of the proposed methodology for obtaining final gate CD distribution.

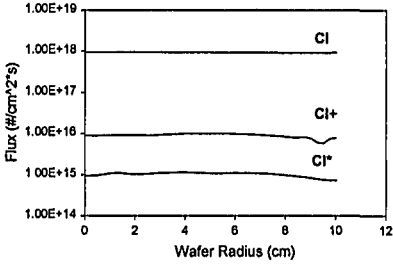


Figure 2: Simulated radial dependence of Cl and Cl+ for the Cl chemistry inductively coupled plasma reactor. Power is 300 W.

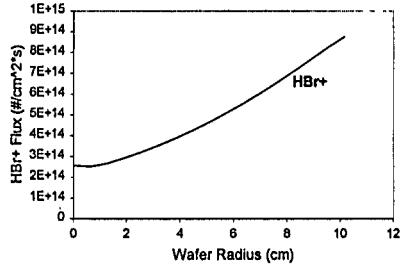


Figure 3: Simulated radial dependence of HBr+ for Cl/HBr chemistry inductively coupled plasma reactor.

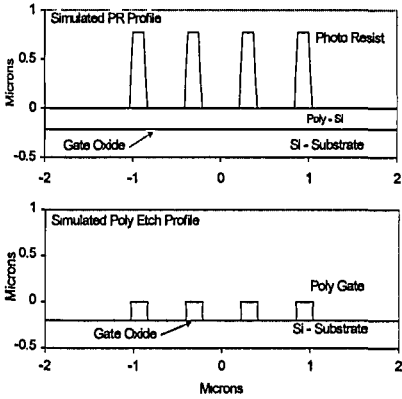


Figure 4: Dense line profiles from lithography simulator (top), and etched poly lines from etch profile simulator (bottom).

| | |
|------------------|----------|
| Mean Value | 179.6 nm |
| St. Dev. | 13.09 nm |
| Focus Variation | 46.6% |
| Exposure Dose | 9.8% |
| PR Thickness | 0.2% |
| BARC Thickness | 0.2% |
| PEB Temperature | 22.9% |
| Development | 3.0% |
| Plasma Variation | 11.8% |
| Reactor Power | 5.3% |
| Overetch Time | 0.2% |

Table 1: Mean and standard deviation of final CD and the contribution to the final CD variance from each process component

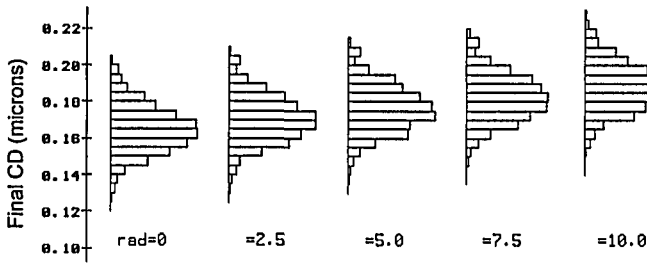


Figure 5: Distribution of final CDs as a function of wafer radius.